pH Dependence of the Reaction Catalyzed by Avian Mitochondrial Phosphoenolpyruvate Carboxykinase†

Todd Holyoak‡ and Thomas Nowak*

Department of Chemistry and Biochemistry, University of Notre Dame, Notre Dame, Indiana 46556

Received February 9, 2004; Revised Manuscript Received April 5, 2004

ABSTRACT: The pH dependence of the reaction catalyzed by phosphoenolpyruvate carboxykinase (PEPCK) provides significant insight into the chemical mechanism. The pH dependence of k_{cat} shows the importance of two acidic ionizations with pK_a values of 6.5 and 7.0 assigned to the active site metal ligands H249 and K228. A single basic ionization is observed with an apparent pK_a value of 8.4 that is assigned to K275 that is located in the P-loop motif and is essential for phosphoryl transfer. The pH dependence of $k_{cat}/K_{M,PEP}$ demonstrates the importance of the same two acidic ionizations in the interaction of phosphoenolpyruvate with PEPCK and a single basic ionization with a pK_a value of 8.1 that is assigned to Y220. The interaction of Mg−IDP with PEPCK is dependent upon a single acidic ionization attributed to K228 and two basic ionizations, both having an average pK_a value of 8.1. One of the basic ionizations is attributed to the P-loop lysine (K275) and the other to C273.

Phosphoenolpyruvate carboxykinase [GTP/ITP:oxaloacetate carboxylase (transphosphorylating; EC 4.1.1.32) (PEPCK)[1]] catalyzes the reversible decarboxylation of oxaloacetic acid with the concomitant transfer of the γ-phosphate of GTP (or ITP) to form PEP and GDP (IDP) as illustrated in Scheme 1. The primary role of the enzyme in most organisms is the

Scheme 1

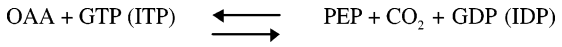

formation of PEP in the first committed step of gluconeogenesis. The protein studied herein is that isolated from chicken liver mitochondria, which has been shown to be a monomeric protein of 67 kDa (*1*).

PEPCK has been isolated and studied from a variety of sources. PEPCK occurs in the cytosol of the adult rat, mouse, and hamster liver (*2*) and in the mitochondria of adult pigeon and chicken (*3*, *4*). PEPCK occurs in both cytosolic and mitochondrial forms in rabbit, pig, and human liver (*2*, *5*−*7*). The cytosolic and mitochondrial forms are distinct proteins and can be distinguished from each other biochemically. The sequences of GTP-utilizing PEPCKs from several sources have been elucidated and are found to contain approximately 60−65% identity among all sources. An additional class of PEPCK exists in *Escherichia coli*, C-4 plants, and yeast. These are mostly multimeric enzymes and utilize ATP rather than GTP (ITP) as the phosphoryl donor. These enzyme forms have been found to have relatively low overall identity with the GTP-utilizing class of enzymes.

Currently little structural information on the chicken mitochondrial isoform of PEPCK exists; however, recently the structure of the homologous human cytosolic enzyme has been determined (*8*). Due to the high degree of similarity between the chicken mitochondrial and human cytosolic enzymes (63% identity), the structural features between the two are likely to be conserved, and therefore the structure of the human cytosolic enzyme is an excellent model for the chicken mitochondrial enzyme. Much of the structural information currently known about the chicken mitochondrial enzyme has arisen from classical chemical modification and inactivation studies and from NMR and EPR techniques to determine active site residues and relative substrate orientations at the active site of the enzyme (*9*−*18*). Additional information has been obtained from the formation of an active Co(III)-PEPCK species that suggested the identity of the activating metal (site I) ligands includes D295 and/or D296 (*19*, *20*). D296 is confirmed to be a metal ligand from the crystal structure of human cPEPCK (*8*).

Previous inactivation studies of the mitochondrial form of PEPCK from chicken liver (*17*) and the cytosolic form from rat liver (*21*, *22*) have indicated that there is a reactive cysteine residue at the active site of PEPCK. Studies on the mitochondrial isoform from this laboratory have suggested that this cysteine is too distant from the active site to be involved in catalysis (*17*), and the structure of the human cytosolic enzyme again confirms the lack of a direct catalytic role for this cysteine (*8*). In addition, it has been shown that

† This research was supported in part by a grant from the National Institutes of Health (DK17049) to T.N. and by the Department of Chemistry and Biochemistry, University of Notre Dame.

* Corresponding author. Phone: (574) 631-5859. Fax: (574) 631-3567. E-mail: Nowak.1@nd.edu.

‡ Current address: Rosenstiel Basic Medical Sciences Research Center, Brandeis University, Waltham, MA 02454.

[1] Abbreviations: ATP, adenosine 5′-triphosphate; cPEPCK, cytosolic phosphoenolpyruvate carboxykinase isoform; DEPC, diethyl pyrocarbonate; EPR, electron paramagnetic resonance; GDP, guanosine 5′-diphosphate; GTP, guanosine 5′-triphosphate; IDP, inosine 5′-diphosphate; ITP, inosine 5′-triphosphate; MDH, malate dehydrogenase; mPEPCK, mitochondrial phosphoenolpyruvate carboxykinase isoform; NADH, nicotinamide adenine dinucleotide, reduced form; NDP, nucleotide 5′-diphosphate; NMR, nuclear magnetic resonance; OAA, oxaloacetic acid; PEP, phosphoenolpyruvate; PEPCK, phosphoenolpyruvate carboxykinase; PRR, water proton longitudinal relaxation rate.

10.1021/bi049707e CCC: $27.50
Published on Web 05/08/2004

modification of a single histidine (*13*), arginine (R289) (*14*, *18*), or lysine (*12*) residue results in the loss of catalytic activity in the mitochondrial form of the enzyme.

To further characterize the role of proposed active site residues in the catalytic mechanism of the PEPCK-catalyzed reaction, the pH dependence of several steady-state kinetic parameters was investigated. The pH dependence of the inactivation rates of cysteine and arginine modification was performed to determine whether these previously determined important residues were reflected in the pK_a values elucidated in the pH studies of steady-state parameters. The ionization of the substrates for the reaction was also investigated by NMR. EPR and PRR spectroscopies were used to investigate the pH dependence on the water coordination of the activating metal (Mn^{2+}) and its binding constant.

MATERIALS AND METHODS

Materials. Malate dehydrogenase was purchased from Boehringer Mannheim Corp. IDP, PEP, NADH, iodoacetic acid, and 2,3-butanedione were purchased from Sigma. All other reagents were of the highest purity available.

PEPCK Purification. Chicken liver PEPCK was purified as previously described (*15*). The concentration of PEPCK was determined using an extinction coefficient $\epsilon_{280}^{1\%} = 16.5 \pm 0.1$ (mg mL)$^{-1}$ (*23*) and a molecular mass of 67000 Da. The enzyme was shown to be >95% pure by SDS−PAGE. The enzyme utilized for these studies had a specific activity of 3.0−6.0 μmol of OAA formed min^{-1} mg^{-1} (units/mg) at 25 °C.

PEPCK Assay. The carboxylation of PEP to form OAA, catalyzed by PEPCK, was assayed by the method of Hebda and Nowak (*23*). In this continuous assay, PEPCK is coupled to MDH, and the disappearance of NADH is continuously monitored with time at 340 nm on a Gilford 240 or 250 spectrophotometer thermostated at 25 °C. The slope was converted to velocity units by using the extinction coefficient of NADH (*24*). The concentration of the substrate CO_2 was calculated from the concentration of substrate added as $KHCO_3$. The concentration of dissolved CO_2 at varying pH values was calculated using the equilibrium constant for dissolved CO_2 and carbonic acid, $K_1 = 1.3 \times 10^{-3}$, and the pK_a values for the ionization of carbonic acid and bicarbonate, p$K_{a1} = 3.7$ and p$K_{a2} = 10.3$, respectively (*25*). These values were used in eq 1 to calculate the concentration of dissolved CO_2 at varying pH.

$$[CO_2(aq)] = \frac{[KHCO_3]}{1 + K_1 + K_1(10^{pH-pK_{a1}}) + K_1(10^{pH-pK_{a1}})(10^{pH-pK_{a2}})} \quad (1)$$

pH Dependence of Steady-State Parameters. The carboxylation of PEP to form OAA was monitored under steady-state conditions as described previously except the initial velocity measurements that were determined in the pH studies were carried out under mixed metal conditions. These conditions use the same PEPCK assay conditions as previously described, but 60 μM $MnCl_2$ and 4 mM $MgCl_2$ were substituted for 4 mM $MnCl_2$ in the standard assay. The rest of the substrates, when kept constant, were 2 mM PEP, 2 mM IDP, and 200 mM $KHCO_3$. The reaction was studied over a pH range of 6.25−9.0 utilizing MES, HEPES, Tris, and TAPS buffers. The buffers were utilized in an overlapping manner. No buffer effects were observed over the pH range studied. An assay mixture containing all of the components except for the variable substrate, PEPCK, MDH, and bicarbonate was prepared and the pH adjusted accordingly. The pH of the bicarbonate solution was adjusted to the same desired pH. An aliquot of the assay mix was then added to a cuvette containing the variable substrate and the appropriate amount of water. The reaction was initiated by the addition of PEPCK. The pH of each assay mix was again determined after the assay to ensure it remained constant over the course of the reaction. The resultant steady-state parameters were analyzed as a function of pH and fit to one of the following equations (*26*):

$$\log y = \log \frac{C_0}{1 + \frac{[H^+]}{K_{a1}} + \frac{[H^+]^2}{K_{a1}K_{a2}} + \frac{K_{a3}}{[H^+]}} \quad (2)$$

$$\log y = \log \frac{C_0}{1 + \frac{[H^+]^2}{(K_{a1,2})^2} + \frac{K_{a3}}{[H^+]}} \quad (3)$$

$$\log y = \log \frac{C_0}{1 + \frac{[H^+]}{K_{a1}} + \frac{(K_{a2,3})^2}{[H^+]^2}} \quad (4)$$

In eqs 2−4, y is the kinetic parameter of interest, C_0 is the pH-independent parameter (k_{cat}, k_{cat}/K_M), $[H^+]$ is the proton concentration, and the K_a values represent the ionization constants for the groups undergoing ionization. Equation 2 defines the kinetic parameter that is affected by three independent ionizations. In eqs 3 and 4, $(K_{a1,2})^2$ and $(K_{a2,3})^2$ represent the product of two ionization constants for groups that are separated by less than 0.6 pK_a unit. The pK_a values for these residues cannot be distinguished and are therefore treated as equivalent ionizations (*26*).

pH-Dependent Inactivation Studies with Iodoacetate and Iodoacetamide. Iodoacetate and iodoacetamide were utilized to modify PEPCK over a pH range of 6−9 utilizing potassium phosphate buffer. PEPCK was initially treated with Chelex-100 resin and desalted by centrifugation in a Filtron spin column with a 10 kDa exclusion limit. This enzyme (0.5 mg mL^{-1}) was then incubated at room temperature in the presence of 50 mM buffer, 100 mM KCl, and 0.6 mM iodoacetate or 0.6 mM iodoacetamide. An identical solution that contained neither iodoacetate nor iodoacetamide was also prepared as a control. A 20 μL aliquot of the incubation mixture was withdrawn at various time intervals and assayed by the standard PEPCK assay without β-mercaptoethanol. Values for k_{obs} were determined at each pH value from the slope of the data plotted as a first-order process. The log of the inactivation rates was plotted as a function of pH and fit to eq 5 (*26*). In eq 5, Y_L is the rate constant for inactivation at low pH and Y_H is the value at high pH, $[H^+]$ is the proton concentration, and K_a is the dissociation constant for the group undergoing ionization.

$$\log y = \log \frac{Y_L + Y_H\left(\frac{K_a}{[H^+]}\right)}{1 + \frac{K_a}{[H^+]}} \quad (5)$$

Arginine Modification by 2,3-Butanedione. 2,3-Butanedione was utilized to modify PEPCK over a pH range of 6−9 utilizing the same buffers as previously indicated. PEPCK was treated in the same manner as described for the iodoacetate inactivation studies. PEPCK (0.5 mg mL^{-1}) was incubated in the presence of 11 mM 2,3-butanedione (prepared in absolute ethanol), 50 mM buffer, and 100 mM KCl. A similar solution substituting absolute ethanol for the 2,3-butanedione solution was also prepared. A 20 μL aliquot was withdrawn from the incubation mixtures at various time intervals and assayed as described in the iodoacetate studies. Values for k_{obs} and the effect of pH upon inactivation were determined as previously described.

^{31}P NMR Measurements. The ^{1}H-decoupled ^{31}P NMR of IDP and PEP were obtained on a Varian VXR500 NMR at 202.35 MHz. PEP (0.040 M) in 10% D_2O was placed in a 5 mm NMR tube, and the spectrum was obtained at 22 ± 0.5 °C. A total of 120 transients were obtained at each pH value. The pH was adjusted by the addition of either 1 M HCl or 1 M KOH and the pH determined in the NMR tube with a Wilmad 6030-02 pH electrode and a Fisher Accumet pH meter. IDP was treated in an identical fashion except 320 transients were obtained at each pH value. $MgCl_2$ was included to ensure that all IDP existed as the binary Mg−IDP complex. The specific concentrations were 0.02 M IDP and 0.04 M $MgCl_2$. All resonances are relative to an external sample of 85% phosphoric acid (0 Hz). The pH dependence of the chemical shifts was fit to eq 5 to generate pK_a values for each ionizable group.

^{13}C NMR Measurements. The natural abundance ^{13}C NMR of IDP was obtained on a Varian VXR600 NMR at 150.84 MHz. For the titration of IDP, 0.100 M IDP in 10% D_2O was placed in a 3 mm NMR tube and its spectrum obtained at 21 ± 0.5 °C. A total of 1000−3000 transients were obtained at each pH value. The pH was adjusted by the addition of either 1 M HCl or 1 M KOH and the pH determined in the NMR tube with a Wilmad 6030-02 pH electrode and a Fisher Accumet pH meter. For the titration of Mg−IDP, 0.1 M IDP and 0.3 M $MgCl_2$ in 10% D_2O were placed in a 3 mm NMR tube, and the spectrum was obtained at 21 ± 0.5 °C. The sample was treated identically to that for IDP. The pH dependence of the chemical shifts was fit to eq 5 to generate a pK_a value for the ionization.

Proton Relaxation Rate Measurements. The formation of the binary enzyme−Mn^{2+} complex as a function of pH was investigated by PRR techniques (*27*, *28*). The longitudinal relaxation rate ($1/T_1$) of water protons was measured with a Seimco pulsed NMR spectrometer operating at 24.3 MHz using the Carr−Purcell 180°−τ−90° pulse sequence (*29*). Enzyme was treated as previously outlined in the inactivation studies. A 50 μL solution was prepared that contained 50−80 μM enzyme, 100 mM KCl, 50 μM $MnCl_2$, and 50 mM buffer. A similar solution that did not contain enzyme was also prepared. The binary enhancement of the $1/T_1$ of the water protons was determined by titration of the first solution into the second, and the data were analyzed as previously described (*14*, *28*). Upon titration of Mn^{2+} into an aqueous solution, the relaxation rate of water protons is increased due to the presence of a new relaxation mechanism provided by the paramagnetic dipole. The effect is observed on the bulk water due to the exchange of the water coordinated to the metal with bulk solvent. Upon inclusion of a macromolecule that binds the metal, the relaxation rate of the water coordinated to the metal in the E−M complex is enhanced further, primarily due to the increase in τ_c in eqs 7 and 8. The rate enhancement can be observed as an effect on bulk solvent due to the water exchange with the E−M complex. The rate enhancement observed in the presence of the E−M complex compared to the $1/T_1$ in the absence of enzyme is termed the binary enhancement (ϵ_b). A more complete description of the phenomena can be found elsewhere (*14*, *27*, *28*). The effect of pH upon ϵ_b was analyzed according to eq 5. The frequency dependence of the effect of pH upon ϵ_b was analyzed over a frequency range of 10.0−45.3 MHz. The paramagnetic contribution to the relaxation rate, $1/T_{1p}$, was calculated from the difference in relaxation rate between samples in the presence and absence of added Mn^{2+}. This value was normalized by the factor p, where p = [enzyme−Mn^{2+}]/[H_2O], to generate values of $1/pT_{1p}$. Under conditions of fast exchange, $1/pT_{1p} = 1/T_{1M}$. For the temperature dependence of $1/pT_{1p}$, the temperature was controlled by the passage of a cooled stream of nitrogen that was heated via a platinum wire electrode across the sample in the probe. The temperature was controlled to an accuracy of ±1 °C. The observed normalized relaxation rate $1/pT_{1p}$ is related to the hydration number, q, of the metal ion, the relaxation time of the water protons at the metal ion, T_{1M}, and the residence time of the water on the metal, τ_m, as shown in the equation:

$$\frac{1}{pT_{1p}} = \frac{q}{T_{1M} + \tau_m} \quad (6)$$

The Solomon−Bloembergen equation relates the relaxation time T_{1M} to a series of constants C, the electron−nucleus distance r, and the correlation time function f(τ_c)

$$r\ (\text{Å}) = C[T_{1M}f(\tau_c)]^{1/6} \quad (7)$$

where C = 812 for Mn^{2+} as the paramagnetic species and ^{1}H is the observed nucleus. The water proton metal distance r has been determined crystallographically to be 2.87 Å (*30*) and is assumed to be the same in this complex. The correlation time function, f(τ_c), has the form

$$f(\tau_c) = 3\tau_c/(1 + \omega_i^2\tau_c^2) + 7\tau_c/(1 + \omega_s^2\tau_c^2) \quad (8)$$

where ω_i is the proton Larmor frequency and ω_s is the electron Larmor frequency (657ω_i). The correlation time, τ_c, has the form

$$1/\tau_c = 1/\tau_s + 1/\tau_m + 1/\tau_r \quad (9)$$

where τ_s is the electron relaxation time, τ_m is the residence time of the water in the coordination sphere of the paramagnet, and τ_r is the rotational correlation time for the enzyme−Mn^{2+} complex. The electron relaxation rate is described by the equation (*25*):

$$1/\tau_s = B[\tau_v/(1 + \omega_s^2\tau_v^2) + 4\tau_v/(1 + 4\omega_s^2\tau_v^2)] \quad (10)$$

Table 1: pH Dependence of Steady-State Parameters for the PEPCK-Catalyzed Carboxylation of PEP To Yield OAA[a]

kinetic parameter	variable substrate	pH independent value	pK_{a1}	pK_{a2}	pK_{a3}	eq[b]
k_{cat}	PEP	1.68×10^2 min^{-1}	6.24 ± 0.26	7.33 ± 0.27	8.47 ± 0.04	2
k_{cat}	Mg·IDP	2.60×10^2 min^{-1}	6.76 ± 0.04	6.76 ± 0.04	8.30 ± 0.08	3
k_{cat}	CO_2	2.23×10^2 min^{-1}	6.36 ± 0.24	7.14 ± 0.25	8.40 ± 0.06	2
k_{cat}/K_M	PEP	1.43×10^6 M^{-1} min^{-1}	7.26 ± 0.05	7.26 ± 0.05	8.08 ± 0.11	3
k_{cat}/K_M	Mg·IDP	1.50×10^6 M^{-1} min^{-1}	7.03 ± 0.17	NA[c]	8.15 ± 0.09	4
					8.15 ± 0.09	
k_{cat}/K_M	CO_2	2.10×10^5 M^{-1} min^{-1}	7.72 ± 0.08	NA	NA	5

[a] The data in panels A and B of Figure 1 are fit to the appropriate equations, and pK_a values are reported. pK_{a1} and pK_{a2} are apparent pK_a values of residues that must be deprotonated for maximal activity while pK_{a3} is the pK_a for residues that must be protonated. [b] The appropriate equation in the text that was used based on the number of pK_a values and the best fit of the data. [c] NA = not applicable.

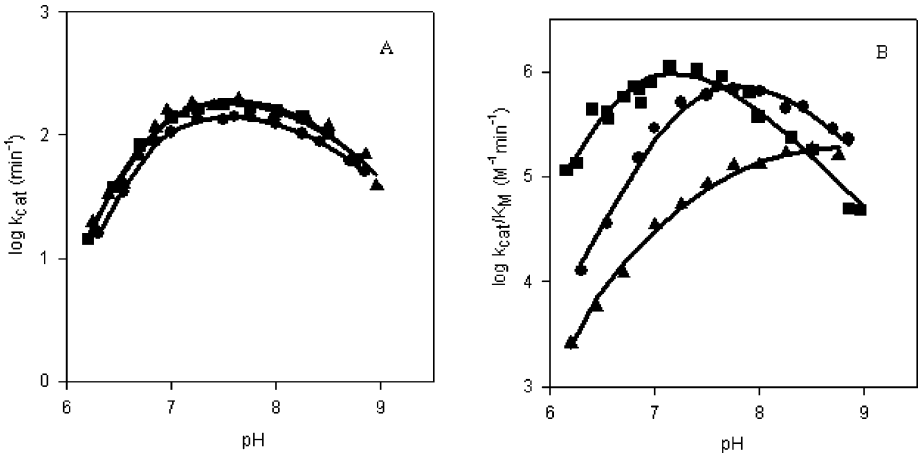

FIGURE 1: pH dependence of steady-state parameters for the carboxylation reaction catalyzed by PEPCK. k_{cat} and K_M were obtained at each pH value by measuring the activity at various concentrations of the variable substrate. The kinetic parameters at each pH were determined from a least-squares fit of the data to the Michaelis−Menten equation. In (A) k_{cat} is plotted as a function of pH with PEP (●), IDP (■), and CO_2 (▲) used as the variable substrate. In (B) k_{cat}/K_{PEP} (●), k_{cat}/K_{IDP} (■), and k_{cat}/K_{CO_2} (▲) are plotted as a function of pH. The curves represent a best fit to the data by a least-squares fit of the appropriate equations (eqs 2−5). The fitted parameters are summarized in Table 1.

where B is a constant that reflects the electron spin and zero field splitting of Mn^{2+} and is a function of the anisotropy of bound Mn^{2+}. The value τ_v is the correlation time for the symmetry distortion at the metal and is attributed to solvent impact. The treatment of such results has been discussed in detail elsewhere (*27*, *28*, *31*).

Electron Paramagnetic Resonance Spectroscopy Measurements. The binding of Mn^{2+} to PEPCK as a function of pH was determined utilizing EPR techniques (*32*). PEPCK was treated with Chelex-100 and desalted as previously described. The enzyme (50−80 μM) was incubated in the presence of 50 mM buffer, 100 mM KCl, and varying concentrations of $MnCl_2$. The binding of Mn^{2+} to the enzyme was measured by EPR. The pH dependence of binding was analyzed by eq 5.

RESULTS

Effect of pH on Steady-State Parameters. The influence of pH on steady-state parameters (k_{cat} and k_{cat}/K_M) was examined to determine the apparent pK_a values of functional groups on the enzyme and substrates that are important in catalysis and enzyme−substrate complex formation. Care must be taken when determining pK_a values from the pH dependence of steady-state parameters as these values can deviate from intrinsic pK_a values due to such factors as the relative rates of specific steps in the catalytic mechanism and the environment of the E−S complex (*33*). The reaction was studied in the direction of the carboxylation of PEP to form OAA and ITP. Initial studies that utilized Mn^{2+} as the source of metal for both the enzyme and the nucleotide resulted in precipitation at basic pH. This precipitation limited the study to a maximum pH of 8. To resolve this problem, a mixed metal assay, as described, was utilized. Conditions were chosen such that the high concentration of magnesium results primarily in the Mg−NDP complex while the manganese preferentially forms the active binary PEPCK−Mn^{2+} complex. mPEPCK binds Mn^{2+} 3 orders of magnitude tighter than it binds Mg^{2+} (*16*). These conditions allowed the enzyme to be studied over a pH range of 6.2−8.9. The limitation at low pH is due to catalytic sensitivity. Overlap of buffers was utilized, and no effect upon the kinetic parameters was observed upon buffer substitution. The individual pH profiles are illustrated in Figure 1. The data are fit with the appropriate equations (eqs 2−5) that model one to three ionizations and whether the pK_a values are separated by <0.6 pH unit or not. The calculated pK_a values from all of the data are summarized in Table 1. No effect on the kinetic constants k_{cat} or K_M was observed upon a doubling of the apparent viscosity of the assay by inclusion of sucrose (data not shown).

There is a similar pH dependence of k_{cat} (Figure 1A) regardless of the variable substrate. The equivalence of the three profiles confirms that the fixed substrates are indeed saturating. In each case, there are three important ionizations in the ES complex. Two residues with apparent pK_a values of approximately 6.3 and 7.2 need to be deprotonated while

a single ionization with an apparent pK_a of 8.4 needs to be protonated for optimal activity.

Examination of the results from k_{cat}/K_M profiles (Figure 1B) reveals several ionizations that appear to be important in the "free enzyme" [2] (E) or in the free substrate (S) to form the respective "ES" complex. From a fit of the data for $k_{cat}/K_{M,PEP}$, it is observed that three ionizations are important for substrate−enzyme interaction. Two residues must be deprotonated. Since the two ionizations that must be deprotonated are separated by less than 0.6 pH unit, the values are assumed to be identical and are fit to eq 3 (*26*). The fit yields two pK_a values of 7.3. A single residue with an apparent pK_a value of 8.1 must be protonated for optimal interaction.

In the case of $k_{cat}/K_{M,Mg\cdot IDP}$, a model that generates a pH dependence on three residues is utilized to generate a best fit to the data. A single acidic ionization with a pK_a value of 7.0 is calculated from the fit of the data. Two basic ionizations, separated by less than 0.6, are observed, and the data are fit to eq 4. The two basic ionizations have an average calculated pK_a value of 8.2.

From a similar analysis of the pH dependence on $k_{cat}/K_{M,CO_2}$, a best fit of the data to a model where complex formation is dependent on a single ionization (eq 5) generates an apparent pK_a value of 7.7 for a residue that must be deprotonated.

Effect of pH on the Rate of Inactivation by Iodoacetate and Iodoacetamide. Previous studies of mitochondrial PEPCK have revealed that treatment of PEPCK with thiol modification agents such as iodoacetate and iodoacetamide leads to inactivation of the enzyme (*17*). A pH study of the rate of inactivation by iodoacetate and by iodoacetamide and a comparison with the pK_a values from the kinetic studies could provide insight into whether this cysteine is relevant to catalysis. The rate of inactivation of PEPCK by each of the reagents was carried out as described over a pH range of 6−9. Pseudo-first-order kinetics of inactivation were observed from the linear nature of the semilog plots. The rate constant for inactivation at each pH value was determined from the slopes of the plots (data not shown). A replot of the observed rate constants for inactivation with respect to pH is shown in Figure 2. The best fit of inactivation data with iodoacetate to eq 5 generates a pK_a value of 7.83 ± 0.11 with a limit to the observed pseudo-first-order reaction rate constant of 0.08 min^{-1} at low pH increasing to 0.55 min^{-1} at high pH. The same experiment was performed with 0.60 mM neutral iodoacetamide. Similar pH-dependent inactivation was obtained with limiting pseudo-first-order rate constants of 0.007 min^{-1} and 0.88 min^{-1} at low and high pH, respectively. A fit to the data by eq 5 gave a similar pK_a value of 8.24 ±0.10 (data not shown).

pH Dependence of the Rate of Inactivation by 2,3-Butanedione. Previous studies (*14*) have revealed the existence of a single arginine residue that is important for catalysis. The pH dependence of the rate of inactivation of PEPCK by 2,3-butanedione, a modification agent specific for arginine, was investigated over the pH range of 6−9. The rates of inactivation followed pseudo- first-order kinetics, and the individual rate constants were calculated from the slopes of the plots (data not shown). A replot of k_{inact} as a function of pH is shown in Figure 3. A fit of the data to eq 5 generates a pK_a value of 7.42 ± 0.14 with a limit to the observed pseudo-first-order reaction rate constant of 0.03 min^{-1} at low pH increasing to 0.2 min^{-1} at high pH.

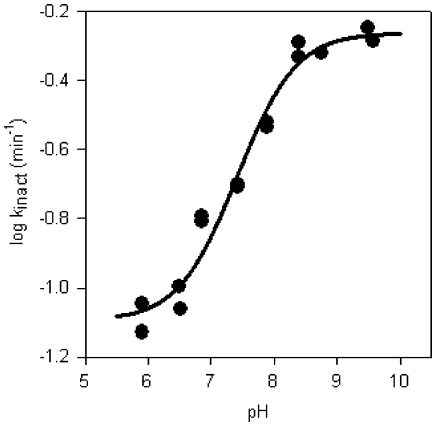

FIGURE 2: pH dependence of the rate constant for inactivation of PEPCK by iodoacetate. PEPCK (0.5 mg mL^{-1}) was incubated in the presence of 0.625 mM iodoacetate as outlined in Materials and Methods. Samples were withdrawn at various time periods and tested for remaining activity. The inactivation rate constant (k_{inact}) was determined from the slopes of the lines using a least-squares fit to the data (data not shown). The log of the resulting inactivation rate constant (k_{inact}) is plotted against the pH of the incubation mix. The curve represents a least-squares fit of the data to eq 5. This generates a pK_a of 7.83.

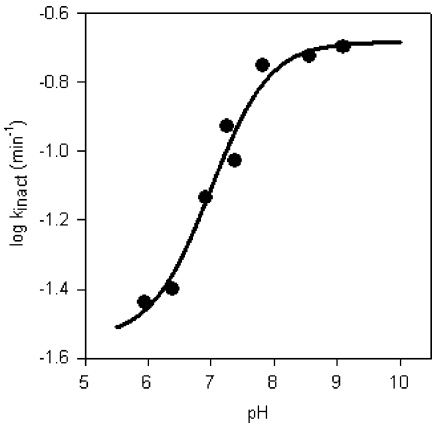

FIGURE 3: pH dependence of the rate constant for inactivation of PEPCK by 2,3-butanedione. PEPCK (0.5 mg mL^{-1}) was incubated in the presence of 2,3-butanedione (11 mM) as outlined in Materials and Methods. Samples were withdrawn at various time periods and tested for remaining activity. The inactivation rate constant (k_{inact}) was determined from the slopes of the lines using a least-squares fit to the data (data not shown). The log of the resulting inactivation rate constant (k_{inact}) is plotted against the pH of the incubation mix. The curve represents a least-squares fit of the data to eq 5. This generates a pK_a of 7.42.

pH Dependence of the ^{31}P Chemical Shifts of PEP and IDP. The pK_a values of the phosphate groups of the substrates for the reaction were determined to elucidate if any of the ionizations that appear in the steady-state kinetic profiles may be due to ionizable groups of the substrates. These ionizable groups may be essential for binding and catalysis. The ^{31}P NMR spectra of PEP and IDP were determined at 202.35 MHz as described in Materials and Methods. The nucleotide existed primarily (97%) as the Mg−IDP complex, based on the reported K_D for the complex (*15*). The positions of the respective resonances of the α- and β-phosphates of IDP and the phosphate of PEP were monitored as a function of

[2] Free enzyme in this instance represents the enzyme complex without the variable substrate.

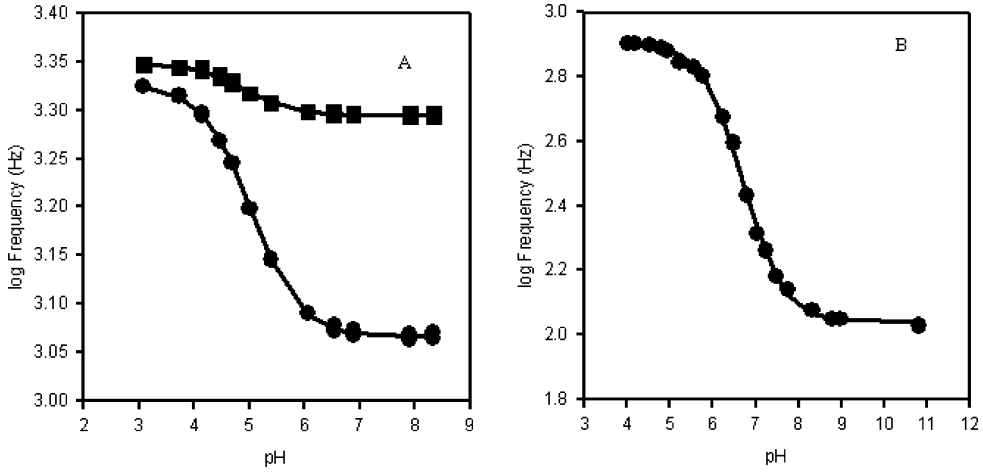

FIGURE 4: pH dependence of the chemical shift of the phosphate resonances of Mg−IDP and of PEP as determined by ^{31}P NMR. The proton-decoupled ^{31}P NMR of IDP and PEP were determined on a Varian VXR500 NMR at 202.35 MHz. A solution of 0.04 M PEP was placed in a 5 mm NMR tube in the presence of 10% D_2O, and its spectrum was obtained at 22 ± 0.5 °C. A total of 120 transients were obtained at each pH value. The pH was adjusted by the addition of either 1 M HCl or 1 M KOH and measured in the NMR tube with a Wilmad 6030-02 pH electrode and a Fisher Accumet pH meter. The IDP sample was treated in an identical fashion except 320 transients were obtained at each pH value. $MgCl_2$ was included to ensure that IDP existed as the binary Mg−IDP complex. The specific concentrations were 0.02 M IDP and 0.04 M $MgCl_2$. All resonances are relative to an external sample of 85% phosphoric acid (0 Hz). The log of the chemical shifts are plotted as a function of pH. The curves represent the calculated best fit to the data by a least-squares fit using eq 5. (A) Log of the chemical shifts (Hz) versus pH for the α-phosphate (●) and the *β*-phosphate (■) of IDP. The fit to the data by eq 5 generates a pK_a value of 4.9 for both the α- and *β*-phosphate of Mg−IDP. (B) Log of the chemical shifts (Hz) versus pH for the phosphate group of PEP. The fit to the data by eq 5 generates a pK_a value of 6.29.

Scheme 2: Ionization of the Inosine Ring of IDP at Basic pH

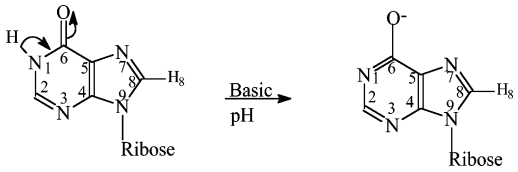

added base or acid, and the pH was determined at each addition of acid or base. The results are presented in Figure 4. The data were fit to eq 5, and the pK_a values generated were 4.85 ± 0.01 for Mg−IDP as measured from the titration of both the α- and *β*-phosphates of Mg−IDP (Figure 4). The second ionization of the phosphoryl group of PEP is 6.29 ± 0.02.

pH Dependence of the ^{13}C Resonances of IDP. At basic pH, IDP has the propensity for ionization of the C-6 carbonyl to generate the enolate as illustrated in Scheme 2. To determine the pK_a value for this ionization under the conditions of the experiments, the ^{13}C spectra of IDP were obtained at various pH values. The C-6 resonance for IDP demonstrated a large pH-dependent shift. A fit of the change in chemical shift with pH to eq 5 generates a pK_a value of 9.03 ± 0.01 (Figure 5). The other carbon atoms in the heterocyclic ring show the same pH transition that titrates with an identical pK_a value. The magnitudes of the chemical shift changes of the other resonances are much smaller than that of the C-6 carbon (data not shown). Since Mg−IDP is the substrate for the reaction and the competent form of the nucleotide used for the steady-state kinetics, IDP was incubated with a 3-fold excess of $MgCl_2$. The pH dependence of the resonance positions was determined for this complex. This study was limited to pH values below pH 9 since insolubility problems were encountered above this pH. Incorporation of Mg^{2+} in the sample had no effect on the resonance positions at low pH so the chemical shift at basic pH, determined from the IDP sample, was utilized to fit the

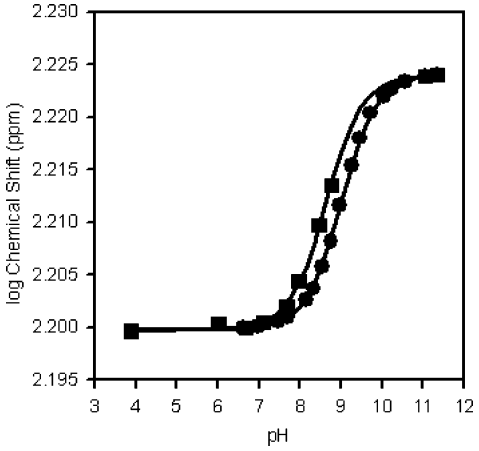

FIGURE 5: pH dependence of the chemical shift of the ^{13}C resonances of IDP as determined by ^{13}C NMR. The ^{13}C NMR spectrum of IDP was obtained on a Varian VXR600 NMR at 150.84 MHz. A total of 1000−3000 transients were obtained at each pH value. The pH was adjusted by the addition of either 1 M HCl or 1 M KOH, and the pH was measured in the NMR tube with a Wilmad 6030-02 pH electrode and a Fisher Accumet pH meter. The samples were either 0.10 M IDP (●) or 0.10 M IDP and 0.30 M $MgCl_2$ (■). Each sample contained 10% D_2O, and the temperature was 21 ± 0.5 °C. The pH dependence of the chemical shifts was fit to eq 5 to generate pK_a values for the transitions, and a pK_a value of 9.03 for IDP was calculated. Incorporation of Mg^{2+} in the sample had no effect on the resonance position at low pH so the basic limit determined from the IDP sample was utilized to fit the Mg−IDP data. A fit to the data by eq 5 generates a pK_a value of 8.65.

Mg−IDP data. A fit to these data by eq 5 generates a pK_a value of 8.65 ± 0.01 (Figure 5).

Investigation of the Metal Binding Site as a Function of pH by PRR. The paramagnetic nature of Mn^{2+}, used as the activating cation in the case of PEPCK, allows for the use of a low-field NMR technique to investigate the proton relaxation rates (PRR) of the bulk water in solution. These data reflect information about the environment of the metal

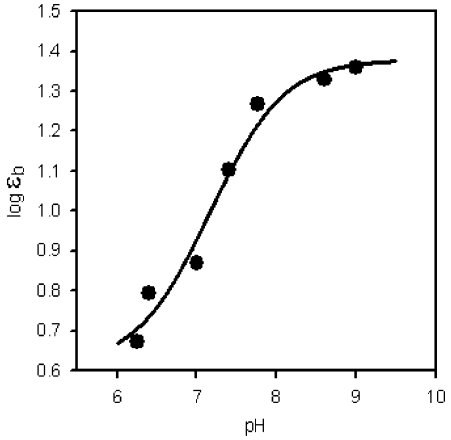

FIGURE 6: pH dependence of the binary enhancement (ϵ_b). The binary enhancement was determined at each pH value by a PRR titration of apo-PEPCK with an identical solution containing Mn^{2+}. The binary enhancement was determined as previously described. The log of the binary enhancement is plotted as a function of pH. The curve represents the best fit to the data by a least-squares fit to eq 5. The pK_a generated is 7.55.

Table 2: Values for $1/pT_{1p}$ as a Function of pH and Frequency

	$1/pT_{1p}$ ($\times 10^{-7}$ s^{-1})				
pH	10 MHz	13.5 MHz	24.3 MHz	35.3 MHz	45.3 MHz
6.5	2.14	1.92	2.46	1.59	1.19
7.0	2.69	2.86	2.98	2.15	1.64
7.5	2.92	3.00	3.36	2.33	1.76
8.0	2.50	3.05	3.31	2.30	2.32
8.5	2.45	3.10	3.27	2.37	1.92
9.0	3.19	3.92	4.07	3.18	2.63

when bound to the enzyme. PRR has been used extensively by this and other laboratories to investigate the metal binding sites of numerous metal-requiring enzymes including PEPCK (*27*, *28*). In an effort to determine if pH has any effect upon the environment surrounding the activating metal binding site, the binary enhancement of the relaxation rate of water molecules upon binding of the metal to the enzyme (*28*) was analyzed as a function of pH. The binary enhancement (ϵ_b) increases with an increase in pH (Figure 6). The data were fit to eq 5, and a best fit to the data generates a pK_a value of 7.55 ± 0.15. Two possible explanations can account for the observed results. Either (i) the number of water molecules coordinated to the metal ion is increased upon progressing from low to high pH or (ii) the number of water molecules undergoing fast exchange is increased by increasing pH. To further investigate the phenomenon, a frequency dependence of $1/pT_{1p}$ as a function of pH was undertaken. By examining the value of $1/pT_{1p}$ at several frequencies, the hydration number of the metal (q) can be estimated (Tables 2 and 3, Figure 7). The calculation of q is obtained by fitting the frequency-dependent data by simultaneously solving eqs 6 and 8−10 until a best fit is obtained (data not shown). The results of the fits reveal that the water protons are indeed undergoing fast exchange since T_{1M} is greater than τ_m by 2 orders of magnitude (Tables 2 and 3). The temperature dependence of $1/pT_{1p}$ indicates Arrhenius behavior with an activation energy between 2 and 4 kcal mol^{-1} over the pH range studied (Table 4). This suggests that the Arrhenius behavior results not from conditions of slow exchange but from fast exchange with τ_s dominating τ_c and with τ_s having a positive activation energy (*31*). Using the fitted data, q titrates with pH from a low of 0.45 at pH 6.5 to 0.83 at pH 9.0. Fitting of the data to eq 5 resulted in the determination of a pK_a of 7.23 ± 0.13 for the titration (Figure 7).

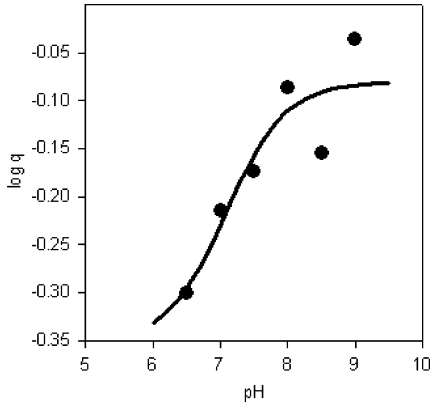

FIGURE 7: pH dependence of the hydration number of the active site Mn^{2+} as determined by the frequency dependence of $1/pT_{1p}$. The log of the calculated hydration number of Mn^{2+} at site I of PEPCK is plotted as a function of pH. The solid curve represents a best fit to the data by a least-squares fit to eq 5. The pK_a generated is 7.23. The value of q titrates from 0.45 at low pH to a value of 0.83 at high pH.

Table 3: Calculated Parameters from Data in Table 2[a]

pH	τ_m ($\times 10^{-9}$ s)	β ($\times 10^{-18}$)	τ_v ($\times 10^{-9}$ s)	q
6.5	11.97	9.1	0.007	0.48
7.0	6.63	5.1	0.012	0.61
7.5	7.93	6.4	0.010	0.67
8.0	4.47	9.0	0.027	0.82
8.5	5.47	789.2	4.12	0.70
9.0	4.50	90.2	5.25	0.92

[a] These parameters were obtained by fitting the frequency dependence of $1/pT_{1p}$ at each pH value as reported in Table 2. In these fits, τ_r is assumed to be the rotational correlation time estimated to be $\tau_r = 33.5$ ns.

Table 4: Activation Energies of Water Relaxation Rates Calculated from Arrhenius Plots of $1/pT_{1p}$ versus $1/T$ (K^{-1})[a]

pH	E_{act} (kcal mol^{-1})
6.5	2.2 ± 0.7
7.5	2.8 ± 0.3
8.0	2.7 ± 0.2
9.0	3.9 ± 0.2

[a] The experiments were performed in the temperature range of 278−308 K.

pH Dependence on the Binding of Mn^{2+} to PEPCK. The pH dependence on the dissociation constant for the binding of Mn^{2+} to PEPCK was determined by EPR spectroscopy. The resultant plot of K_D versus pH is shown in Figure 8. The binding data demonstrate that the metal binds tighter as the pH increases, and the pK_a value for Mn^{2+} binding is 7.32 ± 0.25 from a best fit of the data to eq 5. The K_D value titrates from 40 μM at low pH to 4 μM at high pH.

DISCUSSION

Avian liver mPEPCK has been shown to be inactivated by modification agents that react with histidine, cysteine, arginine, and lysine residues (*13*, *14*, *17*, *18*). The ionization state of several of these residues in the catalytically competent enzyme is obscure; thus their putative roles in catalysis were unknown.

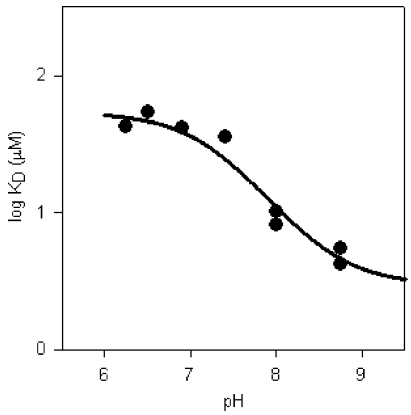

FIGURE 8: pH dependence of the K_D of the active site Mn^{2+} as determined by EPR spectroscopy. The log of the K_D is plotted as a function of pH. The solid curve represents a best fit to the data by a least-squares fit to eq 5. The pK_a value generated is 7.4.

The kinetic mechanism by which mPEPCK operates has recently been elucidated and is found to proceed via a sequential ordered mechanism with PEP binding first followed by IDP and CO_2 (*34*, *35*). The product release steps are also ordered with OAA release preceding that of the nucleotide triphosphate. The lack of an observed viscosity effect on the kinetic parameters (k_{cat} and K_M) provides evidence that substrate association or product dissociation is not rate determining under the conditions of the experiment. On the basis of this knowledge the ionizations observed in the pH profiles of the kinetic parameters should reflect those in the specific complexes as determined by the kinetic mechanism.

The pH dependence of the reaction catalyzed by PEPCK was extended to a pH range of approximately 6−9 by modification of the standard assay to one that contained a mixed metal system. In the assay, the high divalent metal concentration needed to saturate the nucleotide was provided by magnesium, and the activating metal (Mn^{2+}) was kept at a lower concentration but sufficient to saturate the enzyme−metal site. The selectivity of avian mPEPCK for Mn^{2+} is 10^3 greater than it is for Mg^{2+} (*16*). These conditions alleviate the problem of the formation of insoluble Mn^{2+} complexes at higher pH and provided an acceptable range in which both ascending and descending limbs of the pH curves could be defined. The consistency of the k_{cat} profiles (Figure 1) provides evidence that the nonvariable substrates are sufficiently saturating although for technical reasons they may not always be ≥20 times their K_M values.

No three-dimensional structure currently exists for the mitochondrial isozyme of PEPCK, but the human cytosolic isozyme in substrate-free form as well as the PEP and β,γ-methylene-GTP complexes have recently been crystallized (*8*). Since chicken mPEPCK and human cPEPCK have 63% identity, the cPEPCK data will be used as a structural model with which to interpret the origins of the ionizations determined from the kinetic studies.

pH Dependence of k_{cat}: Acidic Ionizations. The k_{cat} profiles, regardless of the variable substrate, show a typical bell-shaped curve that shows a dependence on the deprotonation of two acidic residues and the protonation of one basic residue for maximal activity (Table 1 and Figure 1). On the basis of the crystallographic information (*8*), the DEPC inactivation studies (*13*), and EPR and PRR data, we

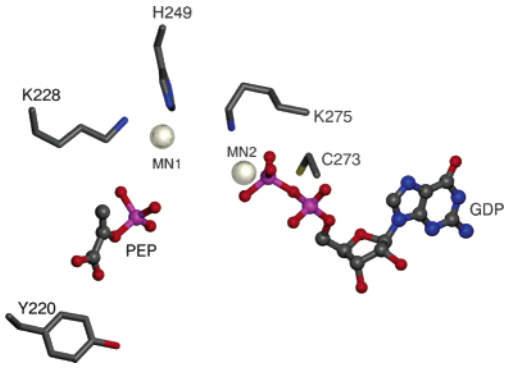

FIGURE 9: Model of the active site of mPEPCK based upon the GTP- and PEP-bound structures of human cytosolic PEPCK (PDB ID codes 1KHB and 1KHF). Those residues whose ionizations are manifest in the kinetic data, the active site metal (MN1), and the nucleotide metal (MN2) along with the substrates PEP and GDP are shown. The figure was generated using POVscript+ (http://www.stanford.edu/~fenn/povscript) (*42*) and rendered using POV-Ray (http://www.povray.org).

suggest that the two acidic ionizations are due to a pH-dependent modulation of the interaction of the active site Mn^{2+} with the enzyme. Specifically, on the basis of the structures of the cPEPCK enzyme, we propose the origins of these two ionizations are H249 and K228 (Figure 9). Several points of evidence support this conclusion. First, in the crystal structure of human cPEPCK it is shown that both H249 and K228 are direct ligands to the catalytic (site I) Mn^{2+} (*8*); therefore, their deprotonated state would be important for the metal−enzyme interaction. This is supported by the EPR data that show tighter metal binding with increasing pH that titrates with a pK_a value similar to that of the acidic pK_a values in the k_{cat} vs pH studies (Table 1, Figures 1 and 8). This is also supported by mutagenic data from the ATP-dependent isozyme in yeast. In the experiments with yeast PEPCK, it was shown that mutation of the corresponding lysine and histidine residues resulted in an increase in the K_D for Mn^{2+} of 30−100-fold, respectively, and a decrease in k_{cat} of 5000-fold (*36*). Further, it seems clear from the pH dependence on ϵ_b and q that an additional water molecule (or proton) undergoes fast exchange at the metal site with increasing pH. This suggests pH-dependent changes in the coordination sphere of the site I metal with an apparent pK_a similar to that determined for the pK_a values of the acidic residues in the steady-state kinetic studies. In addition, the fits to the pT_{1p} data as a function of pH show an increase in the anisotropy factor β with an increase in pH indicating a pH dependence of the electron symmetry in the PEPCK−Mn^{2+} complex consistent with the involvement of additional metal ligands (Table 3). Assignment of H249 to one of the metal ligands not only comes from the crystal structure data (*8*) but also is confirmed by the DEPC inactivation studies that suggest the involvement of a reactive histidine residue ionizing with a similar pK_a to that observed for the acidic ionizations in the kinetic studies (*13*). Recent studies have shown that, in the rat cytosolic enzyme, significant protection from inactivation by DEPC was observed with Mn^{2+} (*37*). A subsequent study of rat cPEPCK inactivation reveals a pK_a value of 7.3 that is similar to the pK_a value generated in the steady-state rate profiles and the PRR and EPR studies for the chicken mitochondrial isoform presented here. Inactivation studies performed on chicken

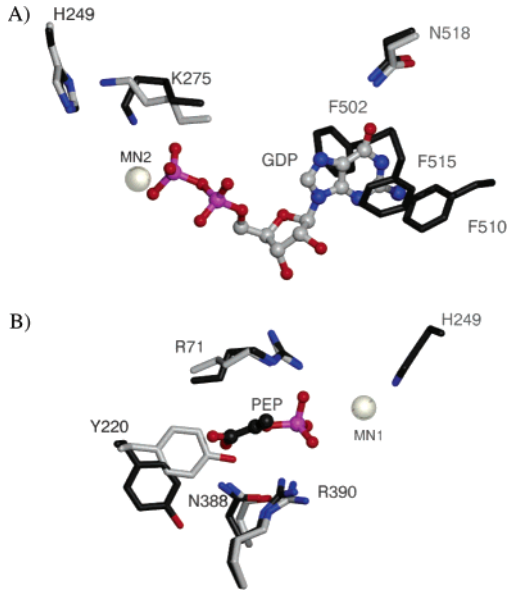

FIGURE 10: Models of the PEP and nucleotide binding sites of human PEPCK (PDB ID codes 1KHB and 1KHF) (*8*). Those residues composing the (A) nucleotide and (B) PEP binding sites are shown, and the residues are numbered according to the sequence of chicken mPEPCK. In the figure the orientation of the residues are shown in the presence (atoms rendered in black) and in the absence of ligand (atoms rendered in gray). The figure was generated using POVscript+ (http://www.stanford.edu/~fenn/povscript) (*42*) and rendered using POVRay (http://www.povray.org).

mPEPCK suggest protection from DEPC inactivation by Mn^{2+}, although not to the extent observed in the case of the rat enzyme. An apparent pK_a of 6.7 for DEPC inactivation of mPEPCK was reported (*13*). Because of the possibilities raised in this study, the raw data from Cheng and Nowak (*13*) were refit to eq 5, and a pK_a of 7.1 was obtained (data not shown). On the basis of these lines of evidence it seems apparent that the two acidic pK_a values observed in the k_{cat} vs pH experiments are due to the ionization of H249 and K228. On the basis of the current experiments, however, it is impossible to assign the individual pK_a values to one residue or the other. These two residues appear to be important in providing the binding site for the site I (catalytic) metal in addition to D296 and one oxygen atom of the γ-phosphate of GTP in that complex (*8*, *11*, *20*). This in turn is essential for the catalytic function of PEPCK presumably through interactions with the phosphoryl group undergoing transfer as has been demonstrated by previous PRR studies (*23*).

pH Dependence of k_{cat}: Basic Ionization. The single basic ionization present in the k_{cat} vs pH studies likely represents the ionization of K275. Lysine residues have always been suggested as possible catalytic residues in the mechanism of PEPCK due to the large amount of negative charge present on the substrates that must be stabilized and the sensitivity of mPEPCK to inactivation by derivatization of lysine residues (*12*). The structures of the PEP and β,γ-methylene-GTP complexes of cPEPCK provide the best additional evidence for the origin of the basic ionization observed in the profile (*8*). These structures show the interaction of K275 with the γ-phosphate of the bound nucleotide tripolyphosphate in that complex while in the apo and PEP complexes, K275 is present in a more extended conformation and is involved in a hydrogen bond with H249 (Figure 10A) (*8*). Additional evidence comes from mutagenic studies with PEPCK from yeast. Although yeast and *E. coli* utilize ATP rather than GTP nucleotides, they have a critical catalytic lysine in the kinase 1a consensus sequence (GX_4GKT) (*38*−*40*). A similar consensus sequence that is completely conserved in the GTP-utilizing PEPCKs has been suggested (*39*), and it is this motif in which K275 is a constituent. This homologous lysine in yeast PEPCK was shown to be critical for phosphoryl transfer by mutagenic studies in which replacement of the lysine with arginine, glutamine, or alanine resulted in a decrease in k_{cat} by 10^4-fold while having no significant effect on K_M for nucleotide or PEP (*38*). The interaction of K275 in a P-loop motif with both the β- and γ-phosphate groups of the nucleotide in the cPEPCK−β,γ-methylene-GTP crystal structure (*8*) supports the idea that K275 functions by helping to neutralize the negative charge buildup in the transition state and to facilitate phosphoryl transfer. A similar lysine interaction with the phosphoryl group of PEP is seen with pyruvate kinase and also serves to stabilize the transition state for phosphoryl transfer (*41*).

pH Dependence of $k_{cat}/K_{M,PEP}$. On the basis of the kinetic mechanism of mPEPCK, the ionizations observed in the $k_{cat}/K_{M,PEP}$ profile should represent those ionizations on the enzyme and substrate important for the interaction of the enzyme with PEP. These experiments generate a bell-shaped curve that is similar to the one generated in the k_{cat} vs pH studies, where the measured parameter is dependent upon the ionization of two acidic residues and one basic residue. On the basis of the explanation above, we believe that the acidic ionizations present in the $k_{cat}/K_{M,PEP}$ profile are attributable to the same residues as implicated in the k_{cat} pH dependence. The geometry and hydration state of the site I metal has previously been shown to be important for the interaction of the substrate PEP with the enzyme (*15*). This is confirmed by the crystal structure data that show the phosphate of PEP interacting with the catalytic metal through an intervening water molecule (*8*, *15*). Therefore, the ionization of the two metal ligands, H249 and K228, would be important for the competent association of PEP with PEPCK. Evidence for the origin of the basic ionization in the k_{cat}/K_M profile for PEP comes again from the structural work on human cPEPCK. In the PEPCK−PEP complex it is shown that the carboxylate of PEP is bound through interactions with the backbone amides of R71 and N388 while the phosphate is coordinated by side chains of R71 and R390 (Figure 10B) (*8*). While none of these residues are expected to be ionizable over the pH range studied, an additional interaction of PEP with Y220 would potentially be pH dependent. Y220 interacts with PEP through an edge-on interaction between the carboxylate oxygen of PEP and the aromatic ring (*8*). In the apo structure, the tyrosine hydroxyl accepts a hydrogen bond from the side chain amide of N388 (*8*). Upon PEP binding the tyrosine is displaced by the caboxylate of PEP, and the hydrogen bond between Y220 and N388 is broken and is replaced by a hydrogen bond between the tyrosine hydroxyl and the main chain carbonyl of N388 (Figure 10B) (*8*). Therefore, upon ionization of the phenolic oxygen of Y220 the apo orientation of Y220 would be stabilized with concomitant destabilization of the PEP-bound conformation. On the basis of the structural rearrangement of Y220 upon the binding of PEP to the enzyme, it is most likely that the residue with an apparent pK_a of 8.1

in the *V*/*K* profile for PEP is that of Y220. Additional experiments will be necessary to support this argument. The ionization of the phosphate group of PEP ($pK_a = 6.29$) as indicated by the ^{31}P NMR titration data may be too low to show any significant effect in the $k_{cat}/K_{M,PEP}$ vs pH data.

pH Dependence of $k_{cat}/K_{M,IDP}$. On the basis of the kinetic mechanism, ionizations present in the *V*/*K* profiles for IDP would represent ionizations of the IDP substrate and/or the E−PEP complex. While the pH dependence on k_{cat}/K_M for IDP is a typical bell-shaped curve, it differs from the dependence of the two previous kinetic parameters (k_{cat} and $k_{cat}/K_{M,PEP}$) in that it reflects a dependence upon one acidic ionization and two basic ionizations. The acidic ionization is again attributable to one of the site I metal ligands. This ionization likely represents the ionization of K228. Mutagenic studies with yeast PEPCK show that mutation of the corresponding lysine to arginine resulted in a 2-fold increase in the K_M for nucleotide while the corresponding H249Q mutant had no effect upon the K_M (*38*). The structural data show the triphosphate nucleotide interacting directly with the manganese ion, displacing one of the three water molecules that are coordinated in the PEP and apo complexes. It is therefore likely that ionization of K228 affects the interaction of IDP with the E−PEP complex. One of the basic ionizations is again attributed to the ionization of K275. Interaction of the ammonium group of K275 with the β-phosphate of IDP is consistent with K275 acting in a role typical of a lysine in a P-loop motif. The shift of the pK_a determined from the kinetic studies from 8.1 in the "free" enzyme to 8.4 in the catalytically competent enzyme is also consistent with this conclusion. While mutagenesis of the corresponding lysine in yeast PEPCK showed no effect on the K_M of nucleotide, it was shown that a positive charge was required for efficient binding of the nucleotide to the enzyme. The lack of a cationic residue at this position resulted in an order of magnitude increase in the K_D (*38*). The fact that in the avian isozyme the ionization of this residue is manifest in the kinetics may reflect differences in the nucleotide substrates and the kinetic mechanisms for these enzymes.

On the basis of the chemical modification studies with iodoacetate and iodoacetamide it is postulated that the second basic ionization in the $k_{cat}/K_{M,IDP}$ profile is that of the conserved cysteine C273. Many previous reports have noted that, in GTP-utilizing forms of PEPCK, there is a reactive cysteine residue and modification of this residue leads to inactivation of the enzyme (*17*, *21*, *22*). Lewis et al. (*21*) have reported the formation of an intramolecular disulfide by vicinal thiols in the rat liver cytosolic enzyme when treated with 8-azidoguanosine 5′-triphosphate. From this observation, the authors concluded that these thiols were critical catalytic residues. Previous studies in this laboratory demonstrated that chicken liver PEPCK was inactivated by known cysteine modifying agents, and this modification was prevented by the presence of nucleotide (*17*). Additional EPR studies with TEMPO-labeled iodoacetamide determined that the labeled cysteine was greater than 10 Å from the activating metal and was proposed to be too distant to be actively involved in catalysis, but may be involved in nucleotide binding (*17*). This was confirmed by NMR studies that showed the TEMPO moiety of the iodoacetamido-TEMPO-derivatized cysteine was located 6−9 Å from the nucleotide ribose (*37*). While the crystal structure of the cPEPCK isozyme supports the lack of a catalytic function for cysteine residues in catalysis mediated by PEPCK, it also provides structural evidence for the inactivation of PEPCKs via modification of this reactive cysteine. The structure of the GTP-bound form of the enzyme shows that the cysteine corresponding to C273 is not exposed to solvent in the nucleotide complex, but in the apo form of the enzyme it is exposed to solvent. These observations are consistent with the chemical modification studies. Burial of the cysteine also corresponds to a decrease in the mobility of the P-loop, and therefore it is likely that burial of C273 is required for productive binding of the nucleotide (*8*). The data presented here show that the inactivation of the enzyme by iodoacetate and iodoacetamide are pH dependent with an increase in the rate of inactivation with an increase in the thiolate form of cysteine. Chemical modification with iodoacetate ($pK_a = 7.8$) and iodoacetamide ($pK_a = 8.2$) is consistent with a pK_a value of approximately 8.0 for this cysteine (C273). Comparison of these data to the results obtained by steady-state studies (Table 1) shows that the pH dependence of $k_{cat}/K_{M,IDP}$ generates two basic values giving an average pK_a of 8.1, one of which we have already attributed to K275. The other we attribute to C273. Since nucleotide binding as shown in the structure of the β,γ-methylene-GTP−PEPCK complex involves the burial of C273, it is probable that the charged thiolate species would not be able to adopt the buried conformation and thus result in a decrease in the apparent second-order rate constant for interaction of E−PEP with IDP similar to that observed upon cysteine derivatization.

An alternative explanation for the origin of the second ionization observed in the $k_{cat}/K_{M,IDP}$ profiles is suggested by the ^{13}C NMR pH titration of IDP. These data suggest the possibility that the origin of one of the basic ionizations in the k_{cat}/K_M profile for IDP is the C-6 carbonyl (pK_a 8.6) of IDP. A shift in the equilibrium to the enolate form of the inosine ring at high pH could account for a decrease in the affinity of the IDP for the enzyme if specific interactions at the C-6 carbonyl of the nucleotide are important. This is expected for an enzyme that can discriminate between adenosine and guanosine/inosine nucleotides. Examination of the β,γ-methylene-GTP−cPEPCK structure shows that the C-6 carbonyl of the bound nucleotide interacts with the enzyme by accepting a H-bond from F515 and N518 (Figure 10A) (*8*). The observation that a H-bond acceptor is needed at C-6 of the bound nucleotide also supports the absolute selectivity of the GTP class of PEPCK for guanosine and inosine nucleotides. In adenosine nucleotides, there is an amino group at this position that would not be able to function as a good H-bond acceptor. This suggests that this interaction is the selectivity filter of the GTP class of PEPCKs for their nucleotide substrates. From the crystal structure it is also observed that the nucleotide binding pocket is composed of F502 and F510 (Figure 10A) (*8*). While the ionization of the C-6 carbonyl would not affect the hydrogen bond between C-6 and F515 and N518, the burial of the ionized form of the ring in this pocket may be disfavored. The observation that the pK_a of C273 is closer to the pK_a determined by steady-state kinetics than the pK_a for the C-6 carbonyl of IDP suggests that the second basic ionization observed is likely to be C273. Further investigation is needed to clarify this issue.

pH Dependence of $k_{cat}/K_{M,CO_2}$. The pH profile exhibited in the pH dependence on the kinetic parameter $k_{cat}/K_{M,CO_2}$ was unexpected. Previous studies on the inactivation of PEPCK with arginine modification agents demonstrated that R289 was the arginine that was involved in the observed inactivation and this inactivation was inhibited by CO_2. Further kinetic analysis supports its proposed role in binding of CO_2 for OAA formation (*18*). The structures of cPEPCK, however, show the presence of a large number of arginine residues located at the active site whose modification could potentially inactivate the enzyme. R289 is located on the surface of the protein remote from the active site (*8*). Since it is unlikely that the pK_a exhibited in the pH dependence of butanedione modification reflects the intrinsic pK_a of any specific arginine, this pK_a may represent a general electrostatic effect of the active site that changes with pH, allowing more facile derivatization of reactive residues as the pH increases. The similarity between the pK_a from butanedione modification and the pH dependence on $k_{cat}/K_{M,CO_2}$ suggests that the same electrostatic effect upon arginine modification by butanedione also affects CO_2 interaction with the E−PEP−IDP complex. In addition, if the ionizations observed in the inactivation and steady-state studies reflected the ionization of a specific residue, it is unclear why a deprotonated arginine would facilitate the interaction of CO_2 with the enzyme. In the PEPCK-catalyzed decarboxylation of OAA, the proposed role of a cationic group at this position would be to interact with the carboxylate of OAA facilitating its departure, thereby reinforcing the conclusion that the apparent pK_a exhibited in the pH vs $k_{cat}/K_{M,CO_2}$ studies does not represent the ionization of a specific residue.

CONCLUSION

In conclusion, this work provides evidence for ionizations of specific residues that appear to play a role in the acid−base process of the reaction catalyzed by avian mitochondrial PEPCK and, more broadly, enzymes of the GTP-utilizing PEPCK family. The importance of the active site metal ligands H249 and K228 as well as K275, C273, and Y220 is apparent from these studies and is consistent with the putative roles of these groups in PEPCK catalysis and with the data measured.

REFERENCES

1. Utter, M. F., and Kurahashi, K. (1953) Mechanism of Action of Oxalacetic Carboxylase from Liver, *J. Am. Chem. Soc. 75*, 758.
2. Nordlie, R. C., and Lardy, H. A. (1963) Mammalian Liver Phosphoenolpyruvate Carboxykinase Activities, *J. Biol. Chem. 238*, 2259−2263.
3. Gevers, W. (1967) Regulation of Phosphoenolpyruvate Synthesis in Pigeon Liver, *Biochem. J. 103*, 141−152.
4. Chiao, Y. (1976) The Intracellular Localization and Kinetic Properties of Chicken Liver Phosphoenolpyruvate Carboxykinase, Ph.D. Thesis, Case Western Reserve University, Cleveland, OH.
5. Holten, D. D., and Nordlie, R. C. (1965) Comparative Studies of Catalytic Properties of Guinea Pig Liver Intra- and Extramitochondrial Phosphoenolpyruvate Carboxykinases, *Biochemistry 4*, 723−731.
6. Brech, W., Shrago, E., and Wilken, D. (1970) Studies on Pyruvate Carboxylase in Rat and Human Liver, *Biochim. Biophys. Acta 201*, 145−150.
7. Wieland, O., Evertz-Prüsse, E., and Stukowski, B. (1968) Distribution of pyruvate carboxylase and phosphoenol-pyruvate carboxykinase in human liver, *FEBS Lett. 2*, 26−28.
8. Dunten, P., Belunis, C., Crowther, R., Hollfelder, K., Kammlott, U., Levin, W., Michel, H., Ramsey, G. B., Swain, A., Weber, D., and Wertheimer, S. J. (2002) Crystal structure of human cytosolic phosphoenolpyruvate carboxykinase reveals a new GTP-binding site, *J. Mol. Biol. 316*, 257−264.
9. Holyoak, T., and Nowak, T. (2001) Structural investigation of the binding of nucleotide to phosphoenolpyruvate carboxykinase by NMR, *Biochemistry 40*, 11037−11047.
10. Hlavaty, J. J., and Nowak, T. (1998) Chromium(III) modification of the first metal binding site of phosphoenolpyruvate carboxykinase, *Biochemistry 37*, 8061−8070.
11. Hlavaty, J. J., and Nowak, T. (2000) Characterization of the second metal site on avian phosphoenolpyruvate carboxykinase, *Biochemistry 39*, 1373−1388.
12. Guidinger, P. F., and Nowak, T. (1991) An active-site lysine in avian liver phosphoenolpyruvate carboxykinase, *Biochemistry 30*, 8851−8861.
13. Cheng, K. C., and Nowak, T. (1989) A histidine residue at the active site of avian liver phosphoenolpyruvate carboxykinase, *J. Biol. Chem. 264*, 19666−19676.
14. Cheng, K. C., and Nowak, T. (1989) Arginine residues at the active site of avian liver phosphoenolpyruvate carboxykinase, *J. Biol. Chem. 264*, 3317−3324.
15. Lee, M. H., and Nowak, T. (1984) Phosphorus-31 nuclear relaxation rate studies of the nucleotides on phosphoenolpyruvate carboxykinase, *Biochemistry 23*, 6506−6513.
16. Lee, M. H., Hebda, C. A., and Nowak, T. (1981) The role of cations in avian liver phosphoenolpyruvate carboxykinase catalysis. Activation and regulation, *J. Biol. Chem. 256*, 12793−12801.
17. Makinen, A. L., and Nowak, T. (1989) A reactive cysteine in avian liver phosphoenolpyruvate carboxykinase, *J. Biol. Chem. 264*, 12148−12157.
18. Nowak, T., Cheng, K. C., Bazaes, S., and Guidinger, P. (1992) The Location of Active-Site Residues in Mitochondrial Phosphoenolpyruvate Carboxykinase (Pepck), *FASEB J. 6*, A471−A471.
19. Hlavaty, J. J., and Nowak, T. (1997) Formation and characterization of an active phosphoenolpyruvate carboxykinase-cobalt(III) complex, *Biochemistry 36*, 3389−3403.
20. Hlavaty, J. J., and Nowak, T. (1997) Affinity cleavage at the metal-binding site of phosphoenolpyruvate carboxykinase, *Biochemistry 36*, 15514−15525.
21. Lewis, C. T., Haley, B. E., and Carlson, G. M. (1989) Formation of an intramolecular cystine disulfide during the reaction of 8-azidoguanosine 5′-triphosphate with cytosolic phosphoenolpyruvate carboxykinase (GTP) causes inactivation without photolabeling, *Biochemistry 28*, 9248−9255.
22. Lewis, C. T., Seyer, J. M., and Carlson, G. M. (1992) Photochemical cross-linking of guanosine 5′-triphosphate to phosphoenolpyruvate carboxykinase (GTP), *Bioconjugate Chem. 3*, 160−166.
23. Hebda, C. A., and Nowak, T. (1982) The purification, characterization, and activation of phosphoenolpyruvate carboxykinase from chicken liver mitochondria, *J. Biol. Chem. 257*, 5503−5514.
24. Noce, P. S., and Utter, M. F. (1975) Decarboxylation of oxalacetate to pyruvate by purified avian liver phosphoenolpyruvate carboxykinase, *J. Biol. Chem. 250*, 9099−9105.
25. Harris, D. C. (1987) *Quantitative Chemical Analysis*, 2nd ed., W. H. Freeman, New York.
26. Cleland, W. W. (1979) Statistical analysis of enzyme kinetic data, *Methods Enzymol. 63*, 103−138.
27. Mildvan, A. S., and Cohn, M. (1970) Aspects of enzyme mechanisms studies by nuclear spin relazation induced by paramagnetic probes, *Adv. Enzymol. Relat. Areas Mol. Biol. 33*, 1−70.
28. Nowak, T. (1981) in *Spectroscopy in Biochemistry* (Bell, J. E., Ed.) pp 109−135, CRC Press, Boca Raton, FL.
29. Carr, H. Y., and Purcell, E. M. (1954) Effects of Diffusion on Free Precession in Nuclear Magnetic Resonance Experiments, *Phys. Rev. 94*, 630−638.
30. Reuben, J., and Cohn, M. (1970) Magnetic resonance studies of manganese (II) binding sites of pyruvate kinase. Temperature effects and frequency dependence of proton relaxation rates of water, *J. Biol. Chem. 245*, 6539−6546.
31. Dwek, R. A. (1972) Proton Relaxation Enhancement Probes−Applications and Limitations to Systems Containing Macromolecules, *Adv. Mol. Relax. Processes 4*, 1−53.
32. Cohn, M., and Townsend, J. (1954) A Study of Manganous Complexes by Paramagnetic Resonance Absorption, *Nature 173*, 1090−1091.
33. Cleland, W. W. (1982) The use of pH studies to determine chemical mechanisms of enzyme-catalyzed reactions, *Methods Enzymol. 87*, 390−405.

34. Lim, A., A.-C. (1997) Product inhibition studies and equilibrium isotope exchange kinetics on phosphoenolpyruvate carboxykinase, Masters Thesis, University of Notre Dame, Notre Dame, IN.
35. Metchkarova, M. (2001) Kinetic mechanism of avian mitochondrial phosphoenolpyruvate carboxykinase, Masters Thesis, University of Notre Dame, Notre Dame, IN.
36. Krautwurst, H., Roschzttardtz, H., Bazaes, S., Gonzalez-Nilo, F. D., Nowak, T., and Cardemil, E. (2002) Lysine 213 and histidine 233 participate in Mn(II) binding and catalysis in *Saccharomyces cerevisiae* phosphoenolpyruvate carboxykinase, *Biochemistry 41*, 12763−12770.
37. Holyoak, T. (2000) Kinetic, structural and genetic characterization of phosphoenolpyruvate carboxykinase, Ph.D. Thesis, University of Notre Dame, Notre Dame, IN.
38. Krautwurst, H., Bazaes, S., Gonzalez, F. D., Jabalquinto, A. M., Frey, P. A., and Cardemil, E. (1998) The strongly conserved lysine 256 of *Saccharomyces cerevisiae* phosphoenolpyruvate carboxykinase is essential for phosphoryl transfer, *Biochemistry 37*, 6295−6302.
39. Matte, A., Tari, L. W., Goldie, H., and Delbaere, L. T. (1997) Structure and mechanism of phosphoenolpyruvate carboxykinase, *J. Biol. Chem. 272*, 8105−8108.
40. Traut, T. W. (1994) The functions and consensus motifs of nine types of peptide segments that form different types of nucleotide-binding sites, *Eur. J. Biochem. 222*, 9−19.
41. Bollenbach, T. J., Mesecar, A. D., and Nowak, T. (1999) Role of lysine 240 in the mechanism of yeast pyruvate kinase catalysis, *Biochemistry 38*, 9137−9145.
42. Fenn, T. D., Ringe, D., and Petsko, G. A. (2003) POVScript+: a program for model and data visualization using persistence of vision ray-tracing, *J. Appl. Crystallogr. 36*, 944−947.

BI049707E